Available online at www.sciencedirect.com
SCIENCE DIRECT®
International Journal of Solids and Structures 42 (2005) 2145–2159
INTERNATIONAL JOURNAL OF SOLIDS and STRUCTURES
www.elsevier.com/locate/ijsolstr

Dynamic stability of a viscoelastic beam with frequency-dependent modulus

Yan-Shin Shih, Zi-Fong Yeh *

Department of Mechanical Engineering, Chung-Yuan Christian University, Chung-Li, 32023 Tao Yuan, Taiwan, Republic of China

Received 7 August 2003; received in revised form 14 September 2004
Available online 2 November 2004

Abstract

This study presents the dynamic stability of a simply supported, viscoelastic beam subjected to an axially harmonic load. The complex modulus of viscoelastic material is considered to depend on the frequency of parametric loading. Applying Galerkin's method, the governing equation of motion is simplified to the complex form of the Mathieu equation with frequency-dependent coefficients. Then, the boundary of dynamic stability is determined by coupling the numerical binary search procedure and the complex incremental harmonic balance (IHB) method, which are developed in this study. This algorithm is easily, simply and conveniently used to perform computer numerical analysis. The results indicate that the loss factor presents the damping capacity of viscoelastic material. The numerical results reveal that the frequency influences the dynamic stability.

1. Introduction

The dynamic stability of the elastic system has been an important subject in the past years. Most researchers in this area have considered the material to be elastic and to have material properties that are independent of frequency. A book by Bolotin (1964) provided detailed practical information about this topic. Various industries rely on vibration control, so viscoelastic materials, such as rubber and polymers, are widely used. Classical constitutive models of viscoelastic material, such as the Maxwell model, the Voigt model and the standard linear model (Sun and Lu, 1995) are generally applied. In these models, viscoelastic materials have a combination of viscous and elastic characteristics and viscous materials are assumed to be ideal viscous or Newtonian viscous materials. Based on such an assumption, viscous damping is described

* Corresponding author. Tel.: +886 3479 6064; fax: +886 3479 6054.
E-mail addresses: ysshih@cycu.edu.tw (Y.-S. Shih), zfyeh@ms14.hinet.net (Z.-F. Yeh).

0020-7683/$ - see front matter © 2004 Elsevier Ltd. All rights reserved.
doi:10.1016/j.ijsolstr.2004.09.007

Nomenclature

CM	complex modulus
MSE	modal strain energy
FD	fractional derivative
ATF	augmenting thermodynamic fields
ADF	anelastic displacement fields
AHL	augmented Hooke's law
GHM	Golla–Hughes–McTavish
IHB	incremental harmonic balance
a, b, p, q	constants determined by viscoelastic material property
a_k, b_k	coefficients of Fourier series of f_0
$\{a\}$	amplitude vector
$B(\omega_i)$	objective function defined by Eq. (9)
C	unbalanced term due to the increment Δf
$[C]$	matrix, whose elements are shown in Appendix A
$[C_1]$, $[C_2]$	sub-matrix of matrix $[C]$, whose elements are shown in Appendix A
D	loss factor corrected by applied constant axial force F_s, defined by Eq. (5)
D_l	D that corresponds to ω_l
E_r	reference constant static modulus of real part of complex modulus E^* at $\omega_n \approx 0$
$\overline{E}$	$=E_R/E_r$
E^*	complex modulus of viscoelastic material $(=E_R[1+i\beta]=E_R+iE_I)$
E_R	real part of complex modulus
E_I	imaginary part of complex modulus
f	amplitude of the first mode
f_0	current value of f
$f_j(t)$	amplitude of the jth mode
$F(t)$	periodic axial force $(=F_s+F_d\cos\omega t)$
F_s	amplitudes of static force
F_d	amplitudes of dynamic force
G	$=(\overline{E}\cdot P_r^*-F)/(P_r^*-F)$
G_l	G, corresponding to ω_l
i	$\sqrt{-1}$
I	moment of inertia of cross section of beam
j	modal index
L	length of beam
L_0	reference length of beam for defining $\bar{\bar{n}}_r$
m	mass per unit length of beam
$M(\Omega,\lambda,f,\tau,\omega)$	dimensionless complex Mathieu equation defined by Eq. (6)
n_r	natural frequency of lateral vibration of elastic beam with elastic modulus E_r, under constant axial force F_s, defined by Eq. (7)
$\bar{n}_r$	reference parameter used in discussion of influence of static force F_s
$\bar{\bar{n}}_r$	reference parameter used in discussion of influence of length of beam
N	positive integer
p_k	midpoint of interval $[u_k, v_k]$

P unbalanced term due to the increment $\Delta\lambda$
P^* static critical load for elastic beam with elastic modulus E_R
P_r^* static critical load for beam with elastic modulus E_r, defined by Eq. (7)
$\{P\}$ vector, whose elements are shown in Appendix A
$\{P_1\}$, $\{P_2\}$ sub-vector of vector $\{P\}$, elements shown in Appendix A
Q unbalanced term due to the increment $\Delta\Omega$
$\{Q\}$ vector, whose elements are shown in Appendix A
$\{Q_1\}$, $\{Q_2\}$ sub-vector of vector $\{Q\}$, whose elements are shown in Appendix A
R corrective term
$\{R\}$ vector, whose elements are shown in Appendix A
$\{R_1\}$, $\{R_2\}$ sub-vector of vector $\{R\}$, whose elements are shown in Appendix A
t time
$[u_0, v_0]$ $=[\omega_{\min}, \omega_{\max}]$
$[u_k, v_k]$ sub-interval
$w(x,t)$ lateral displacement of beam
$w_j(x)$ normalized eigenfunction of simply supported beam
x axial position along undeflected beam
β material loss factor
$\{\delta f\}$ virtual of f defined by Eq. (17)
Δa_k, Δb_k coefficients of Fourier series of Δf_0
$\{\Delta a\}$ amplitude increment vector of $\{a\}$
Δf increment of variable f
$\Delta\lambda$ increment of variable λ
$\Delta\Omega$ increment of variable Ω
ε tolerance
λ load parameter defined by Eq. (5)
λ_0 current value of variable λ
λ_r load parameter for beam with elastic modulus E_r, defined by Eq. (7)
τ non-dimensional time $(=\varpi t)$
ω frequency of applied force
ω_l frequency of vibration, corresponding to $(\Omega_l(\omega_l), \lambda_l(\omega_l))$
ω_{l-1} frequency of vibration, corresponding to $(\Omega_{l-1}(\omega_{l-1}), \lambda_{l-1}(\omega_{l-1}))$
ω_n frequency of vibration of beam
ω_s natural frequency of lateral vibration of elastic beam loaded by constant axial force F_s, defined by Eq. (5)
$[\omega_{\min}, \omega_{\max}]$ frequency range of complex modulus
Ω reduced frequency of vibration $(=\varpi/\omega_s)$
Ω_0 current value of Ω
$(\Omega_l(\omega_l), \lambda_l(\omega_l))$ any point on instability boundary
$(\Omega_{l-1}(\omega_{l-1}), \lambda_{l-1}(\omega_{l-1}))$ point before $(\Omega_l(\omega_l), \lambda_l(\omega_l))$ on instability boundary
ϖ parametric frequency of vibration $(=\omega/2)$

Operators
Re() real part
Im() imaginary part

$\|\|$	norm
∂	differential operator

Superscript

T	transpose

by a constant, and the dimensionless damping ratio increases with frequency. Representing the internal damping of a viscoelastic material as viscous may generate serious errors. Steidel (1989) pointed out that the actual damping ratio decreases as the frequency increases.

Numerous methods of modeling frequency-dependent viscoelastic materials have been proposed. The dependence of complex modulus (CM) on frequency was often modeled even in the 1980s. Furthermore, Huang et al. (1996), Shen (1995, 1996), and Varadan et al. (1996) exploited the exponential formula for complex modulus developed by Douglas and Yang (1978). Johnson and Kienholz (1981) developed the modal strain energy (MSE) method, which states that the damped structure can be represented in terms of real normal modes of the associated undamped system if appropriate damping terms are inserted into the uncoupled equations of motion. Bagley and Torvik (1983) proposed a fractional derivative (FD) model for the frequency-domain analyses of viscoelastic damping, leading in the time-domain to differential equations of fractional order, which are rather complicated to solve. The method of augmenting thermodynamic fields (ATF) was developed from a study of Lesieutre and Mingori (1990), which based on the introduction of internal variables. Lesieutre and Bianchini (1995) later extended the ATF model, which was originally applicable only to unidimensional problems, to the three-dimensional anelastic displacement fields (ADF). In parallel, Dovstam (1995) proposed an augmented Hooke's law (AHL), but performed only a frequency-domain analysis. Golla and Hughes (1985) and McTavish and Hughes (1993) also developed the Golla–Hughes–McTavish (GHM) model, also based on the introduction of dissipative variables. Yiu's model (1993), Yiu (1994) applied a generalized Maxwell model that provided standard mechanical spring-dashpot configurations and canonical mathematical forms to fit the viscoelastic material properties. This study will apply the frequency-dependent exponential formula for the complex modulus (CM) to model viscoelastic materials.

Szyszkowski and Glockner (1985), Gurgoze (1987), Cederbaum and Mond (1992), and Shirahatti and Sinha (1994) investigated this topic by applying spring-dashpot models, such as Maxwell, Voigt–Kelvin and three-parameter models, to determine the dynamic stability of the viscoelastic beam. In these investigations, the dashpot element was assumed to represent the viscous damping of the viscoelastic material.

Saito and Otomi (1979) investigated the dynamic stability of viscoelastic beams, in which the modulus of elasticity is represented by a complex number, and the loss factor is related to the damping ratio. Kar and Sujata (1991), Kar and Ray (1995), and Ray and Kar (1995) considered the dynamic stability of a cantilevered symmetric sandwich beam, which whose core material is viscoelastic, when subject to a pulsating axial force, using a complex modulus model. In the above papers, the complex modulus was considered to be independent of frequency, and the damping was simulated as a hysteretic damping model.

Stevens and Evan-Iwanowski (1969) and Stevens (1969) presented analytical and experimental results to discuss the effect of the behavior of a viscoelastic material on the instability regions of a column, when the complex modulus of the viscoelastic material is influenced by frequency. Steidel (1989) pointed out that the damping ratio is a constant for hysteretic damping model; increases with frequency for a viscous damping model, and decreases as the frequency of actual damping increases. A frequency-independent complex

modulus of the viscoelastic material makes the damping ratio of typical hysteretic damping constant, but a frequency-dependent complex modulus enables the damping ratio to behave more realistically when the frequency of vibration is varied. Accordingly, a model that involves a frequency-dependent complex modulus captures actual damping more accurately than other models.

Stevens and Evan-Iwanowski (1969) and Stevens (1969) applied the method of perturbation to determine dynamic instability. Lau et al. (1982), presented an incremental harmonic balance (IHB) method to determine the parametric instability of viscous damped columns or beam systems. Pierre and Dowell (1985) implemented the extended IHB method to study the dynamic instability of viscous damped plates. Yuan and Lau (1991) have applied the IHB method to discuss the effect of in-plane load on a nonlinear panel flutter. The IHB method has been successfully applied to determine the dynamic instability of a structural system with viscous damping. This algorithm is easily, simply and conveniently implemented for computer numerical analysis. However, the dynamic stability of a viscoelastic beam with a complex modulus that depends on the frequency, has not been determined using the IHB method.

This study investigates the dynamic instability of a simply support viscoelastic beam subjected to a periodic axial force. However, the IHB procedure becomes complicated because the dependence of the complex modulus on frequency is considered. Therefore, this study develops a procedure for coupling the binary-search method and the complex IHB method, to determine dynamic instability.

2. Equation of motion for a viscoelastic beam

Fig. 1 depicts a straight, simply supported beam of length L, with a uniform cross section. The mass per unit length of the beam is m, and the moment of inertia of the cross section is I. A periodic axial force $F(t) = F_s + F_d \cos \omega t$ is applied at $x = L$ as shown, where ω is the frequency of the applied force; t is the time and F_s and F_d are the amplitudes of the static and dynamic forces, respectively. The lateral displacement of the beam is denoted by $w(x, t)$, where x is the axial position along the undeflected beam. Fig. 1 depicts the coordinate system used in this problem.

The material of this beam is considered to be linearly viscoelastic. Hence, the material properties can be represented by a complex elastic modulus E^*, where $E^* = E_R[1 + i\beta] = E_R + iE_I$. E_R, which is the real part of the elastic modulus that determines the stiffness of the material; E_I, the imaginary part of the elastic modulus that determines the damping capacity of the material, and β, the material loss factor, are functions of the vibrating frequency ω_n (Stevens and Evan-Iwanowski, 1969).

In this study, the beam is at a constant and uniform temperature, so the effect of heat on the material properties can be neglected. Therefore, the complex modulus is a function only of the vibrating frequency (Stevens and Evan-Iwanowski, 1969).

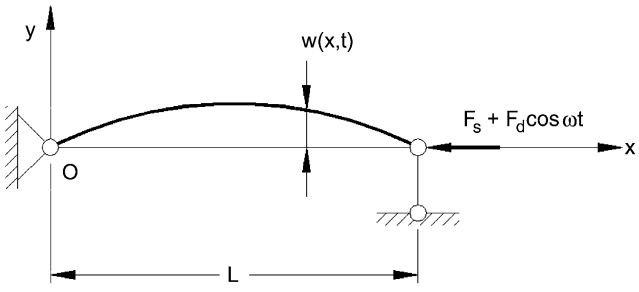

Fig. 1. Simply supported, viscoelastic beam subjected to an axial force.

The thickness is much smaller than the length of the beam, so according to Euler–Bernoulli theory, the effects of shear deformation and rotational inertia can be neglected. The effect of the axial inertia is also negligible. The governing equation of motion is

$$I[E^*]\frac{\partial^4 w}{\partial x^4} + (F_s + F_d \cos \omega t)\frac{\partial^2 w}{\partial x^2} + m\frac{\partial^2 w}{\partial t^2} = 0 \tag{1}$$

The boundary condition of the simply supported beam can be written as

$$w = 0 \quad \text{and} \quad \frac{\partial^2 w}{\partial x^2} = 0 \quad \text{at } x = 0 \text{ and } L \tag{2}$$

The solution to Eq. (1) is assumed to be in the form

$$w(x,t) = \sum_{j=1}^{N} w_j(x) f_j(t) \tag{3}$$

where N is a positive integer; $w_j(x)$ is the normalized eigenfunction of the simply supported viscoelastic beam, given by $w_j(x) = \sin(j\pi x/L)$, and $f_j(t)$ is the amplitude of vibration in the jth mode.

Substituting Eq. (3) into Eq. (1) and applying the generalized Galerkin's method yields a complex Mathieu equation for the first mode

$$\frac{d^2 f}{dt^2} + \omega_l^2[1 + iD - 2\lambda \cos \omega t]f = 0 \tag{4}$$

where

$$\omega_s^2 = \frac{E_R I \pi^4}{mL}\left(1 - \frac{F_s}{P^*}\right); \quad D = \frac{E_I/E_R}{1 - F_s/P^*}; \quad 2\lambda = \frac{F_d}{P^* - F_s}; \quad \text{and} \quad P^* = \frac{E_R I \pi^2}{L^2} \tag{5}$$

Physically, P^* is the critical load that causes the static buckling of an elastic beam with elastic modulus E_R; ω_s is the natural frequency of the lateral vibration of an elastic beam loaded by a constant axial force F_s; D is the loss factor corrected by the applied static load, and λ is the parameter of excitation.

The beam is most likely to vibrate at frequency $\omega/2$ in the principal region of dynamic instability. A set of dimensionless parameters is used, such as the parametric vibration frequency $\varpi = \omega/2$, the reduced vibration frequency $\Omega = \varpi/\omega_s$, and the dimensionless time-scale $\tau = \varpi t$. These variables are used in Eq. (4), the dimensionless complex Mathieu equation; the coefficient function of frequency is

$$M(\Omega, \lambda, f, \tau, \omega) = \Omega^2 \frac{d^2 f}{d\tau^2} + [1 + iD - 2\lambda \cos 2\tau]f = 0 \tag{6}$$

All calculations must be used on some reference value of the modulus to elucidate fully the effect of the dependence of the material properties on the frequency. The quantity $\overline{E} = E_R/E_r$ is introduced, where E_r is a reference constant, which is the static modulus of the real part of the complex modulus E^* at $\omega_n \approx 0$ in this study. The following parameters can be obtained as

$$P_r^* = \frac{\pi^2 E_r I}{L^2}; \quad n_r^2 = \frac{\omega^2}{4\pi^4 E_r I(P_r^* - F_s)/mL^4 P_r^*}; \quad G = \frac{\overline{E} \cdot P_r^* - F_s}{P_r^* - F_s}; \quad \text{and} \quad 2\lambda_r = \frac{F_d}{P_r^* - F_s} \tag{7}$$

Substituting Eq. (7) into Eq. (5), yield

$$P^* = \overline{E} \cdot P_r^*; \quad \Omega^2 = \frac{n_r^2}{G}; \quad \text{and} \quad 2\lambda = \frac{2\lambda_r}{G} \tag{8}$$

Then, the boundary of the dynamic stability is the triplet (f, Ω, λ) solution to Eq. (6) and can be transferred into another form of stability boundary (f, n_r, λ_r).

3. Determining the frequency-dependent coefficient in the complex Mathieu equation

The instability boundary Ω and λ are functions of vibrating frequency, and can be written as $\Omega(\omega_n)$ and $\lambda(\omega_n)$, which can be determined using the incremental harmonic balance method. Each new neighboring state is reached through a parameter increment; a new neighboring point $(\Omega_l(\omega_l), \lambda_l(\omega_l))$ corresponds to vibrate at frequency ω_l and the previous point $(\Omega_{l-1}(\omega_{l-1}), \lambda_{l-1}\ (\omega_{l-1}))$ corresponds to frequency ω_{l-1}. The loss factor parameter D of Eq. (6) also changes.

Accordingly, in each step of the IHB method, the corresponding frequency must to be obtained. This new frequency is used to calculate the corresponding value of the coefficient in Eq. (6).

Assume Ω_l is the known value in the current step; the value in the initial step is set and the values in the other steps are calculated. Substituting Ω_l into $\Omega(\omega) = \omega/2\omega_s$ yields

$$B(\omega_l) = \omega_l^2 - 4 \cdot \Omega_l^2 \cdot \Omega_r^2 \cdot \left(\frac{E_R(\omega_l)}{E_r} - \frac{F_s}{P_r^*}\right) \Big/ \left(1 - \frac{F_s}{P_r^*}\right) = 0 \tag{9}$$

where ω_l is the frequency of the current step that corresponds to Ω_l.

The variation in the complex modulus with frequency is known, so the complex modulus over the frequency interval $[\omega_{\min}, \omega_{\max}]$ is of interest. The binary-search numerical method (Burden et al., 1981) is implemented to search for solution ω_l of Eq. (9) in the frequency interval $[\omega_{\min}, \omega_{\max}]$, for which $B(\omega_l) = 0$. This method calls for a repeated halving of intervals $[\omega_{\min}, \omega_{\max}]$ and, at each step, identifying the half that contains p_k. Initially, set $u_0 = \omega_{\min}$ and $v_0 = \omega_{\max}$. Define a sub-interval $[u_k, v_k]$, and let p_k be the midpoint of interval $[u_k, v_k]$, such that $p_k = (u_k + v_k)/2$. If $B(p_k) \approx 0$, then $\omega_l = p_k$ and the iteration is terminated; if not, continue to apply the process in the new sub-interval $[u_{k+1}, v_{k+1}]$. The iteration is terminated when $|p_{k+1} - p_k| \leqslant \varepsilon$, where ε is a specified tolerance, and $\omega_l = p_{k+1}$.

Substituting ω_l into Eq. (5) determines the frequency-dependent coefficient D_l in Eq. (4). Then, the complex Mathieu equation with the frequency-dependent coefficient is transferred into the complex Mathieu equation with the frequency-independent coefficient. Then, the incremental harmonic balance method is employed to reach the unstable boundary point $(\Omega_l(\omega_l), \lambda_l(\omega_l))$.

Substituting ω_l into Eq. (7) yields G_l, which corresponds to Ω_l. Thereafter, the processor of the incremental harmonic balance method reached the unstable boundary point. Substituting G_l into Eq. (8) yields the unstable boundary point (n_r, λ_r).

4. IHB method for solving the complex Mathieu equation

The procedure for seeking periodic solutions to the Mathieu equation with complex coefficients using the IHB method, includes two steps. The first step is a Newton–Raphson procedure. The current solution to Eq. (6) for λ_0, f_0 and Ω_0, can be increased (by an mount Δ) to yield a neighboring solution,

$$\lambda = \lambda_0 + \Delta\lambda; \quad f = f_0 + \Delta f; \quad \Omega = \Omega_0 + \Delta\Omega \tag{10}$$

Lau et al. (1982) and Pierre and Dowell (1985) detailed the procedure for implementing the IHB method. They modified the IHB method into a complex form.

Expanding Eq. (6) as a Taylor series about the initial state yields

$$\mathrm{M}(\Omega_0+\Delta\Omega,\lambda_0+\Delta\lambda,f_0+\Delta f,\tau,\omega) = \mathrm{M}_0+\left.\frac{\partial \mathrm{M}}{\partial\Omega}\right|_0\Delta\Omega+\left.\frac{\partial \mathrm{M}}{\partial\lambda}\right|_0\Delta\lambda+\left.\frac{\partial \mathrm{M}}{\partial f}\right|_0\Delta f+\text{higher order terms}=0 \tag{11}$$

Neglecting higher order terms yields the linearized incremental equation,

$$C-R-\Delta\lambda\cdot P-\Delta\Omega\cdot Q=0 \tag{12}$$

where

$$C=\Omega_0^2\frac{\mathrm{d}^2\Delta f}{\mathrm{d}\tau^2}+[1+\mathrm{i}D-2\lambda_0\cos 2\tau]\Delta f;\quad P=2f_0\cos 2\tau;\quad Q=-2\Omega_0\frac{\mathrm{d}^2 f_0}{\mathrm{d}\tau^2};\quad \text{and}$$
$$R=-\left\{\Omega_0^2\frac{\mathrm{d}^2 f_0}{\mathrm{d}\tau^2}+[1+\mathrm{i}D-2\lambda_0\cos 2\tau]f\right\} \tag{13}$$

Here, R is the corrective term that goes to zero when the solution is reached, and P and Q are the unbalanced terms, associated with the increments $\Delta\lambda$ and $\Delta\Omega$, respectively.

The second step of the incremental harmonic balance method is the Galerkin procedure. The boundaries of the regions of instability correspond to periodic solutions of Eq. (6) with periods $2\pi/\omega_n$ and $4\pi/\omega_n$. Hence, the functions $f_0(\tau)$ and $\Delta f(\tau)$ are periodic and can be expressed in truncated Fourier series form as,

$$f_0(\tau)=\sum_{k=1,3,5,\ldots}^{2N-1}(a_k\cos k\tau+\mathrm{i}b_k\sin k\tau) \tag{14}$$

$$\Delta f(\tau)=\sum_{k=1,3,5,\ldots}^{2N-1}(\Delta a_k\cos k\tau+\mathrm{i}\Delta b_k\sin k\tau) \tag{15}$$

in the principal region of instability, corresponding to a solution with period 2π in terms of τ. Here, N is the number of temporal terms taken into account. Substituting Eqs. (14) and (15) into Eq. (12), and applying the Galerkin procedure for one period, yields

$$\int_0^{2\pi}C\{\delta f\}\mathrm{d}\tau=\int_0^{2\pi}(R+\Delta\lambda\cdot P+\Delta\Omega\cdot Q)\{\delta f\}\mathrm{d}\tau \tag{16}$$

where

$$\{\delta f\}=[\cos\tau+\sin\tau,\cos 3\tau+\sin 3\tau,\cos 5\tau+\sin 5\tau,\ldots,\cos(2N-1)\tau+\sin(2N-1)\tau]^{\mathrm{T}} \tag{17}$$

Let us define the amplitude vector as $\{a\}=[a_1,\ldots,a_{2N-1},b_1,\ldots,b_{2N-1}]^{\mathrm{T}}$ and its corresponding increment as $\{\Delta a\}=[\Delta a_1,\ldots,\Delta a_{2N-1},\Delta b_1,\ldots,\Delta b_{2N-1}]^{\mathrm{T}}$. Eq. (16) represents N algebraic linear equations in generalized coordinates Δa_ks and Δb_ks. Equating real and imaginary parts derives from Eq. (16) $2N$ algebraic linear equations with real coefficients. These $2N$ algebraic linear equations can be written in matrix form as

$$\begin{bmatrix}[C_1]\\ [C_2]\end{bmatrix}\{\Delta a\}=\begin{Bmatrix}\{R_1\}\\ \{R_2\}\end{Bmatrix}+\begin{Bmatrix}\{P_1\}\\ \{P_2\}\end{Bmatrix}\cdot\Delta\lambda+\begin{Bmatrix}\{Q_1\}\\ \{Q_2\}\end{Bmatrix}\cdot\Delta\Omega \tag{18}$$

where $[C_1]$, $[C_2]$, $\{R_1\}$, $\{R_2\}$, $\{P_1\}$, $\{P_2\}$, $\{Q_1\}$ and $\{Q_2\}$ are as shown in Appendix A. Eq. (18) can be rewritten as

$$[C]\{\Delta a\}=\{R\}+\{P\}\cdot\Delta\lambda+\{Q\}\cdot\Delta\Omega \tag{19}$$

The number of unknowns is two more than the number in Eq. (19). Two constraints, which relate the unknowns $\{\Delta a\}$, $\Delta\Omega$ and $\Delta\lambda$ in Eq. (19), must be added. The boundary of dynamic instability (Ω, λ) of the system is of primary interest, with $\|\{a\}\|$ as a parameter, which is fixed for each curve. Therefore, the first constraint is $\|\{a\}\| = \|\{a\} + \{\Delta a\}\|$. The second constraint is either $\Delta\lambda = 0$ or $\Delta\Omega = 0$. The constraints $\|\{a\}\| = \|\{a\} + \{\Delta a\}\|$ and $\Delta\lambda = 0$ are chosen in this study. Hence, at each step, the following must be solved;

$$\begin{cases} [C]\{\Delta a\} = \{R\} + \{Q\} \cdot \Delta\Omega \\ \|\{a\}\| = \|\{a\} + \{\Delta a\}\| \end{cases} \tag{20}$$

Newton–Raphson iteration with an updated corrective vector $\{R\}$ within an incremental step was applied. The process is repeated until the magnitude of the corrective vector $\{R\}$ is acceptably small, at which point a solution is obtained.

5. Algorithms for determining the boundary of parametric instability of a viscoelastic beam

The complex modulus of a viscoelastic material depends on the vibrating frequency, so the binary-search method must be coupled with the incremental harmonic balance method to determine the boundary of dynamic instability. A boundary of dynamic instability is obtained using the following procedure.

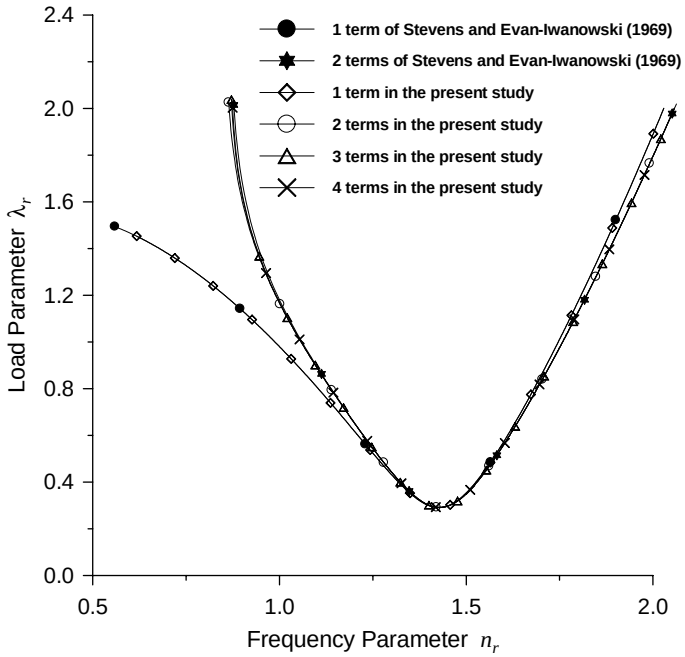

Fig. 2. Influence of the considered number of harmonic terms on the boundary of principal instability and comparison with Stevens and Evan-Iwanowski (1969) for $F_s/P_r^* = 0.6$.

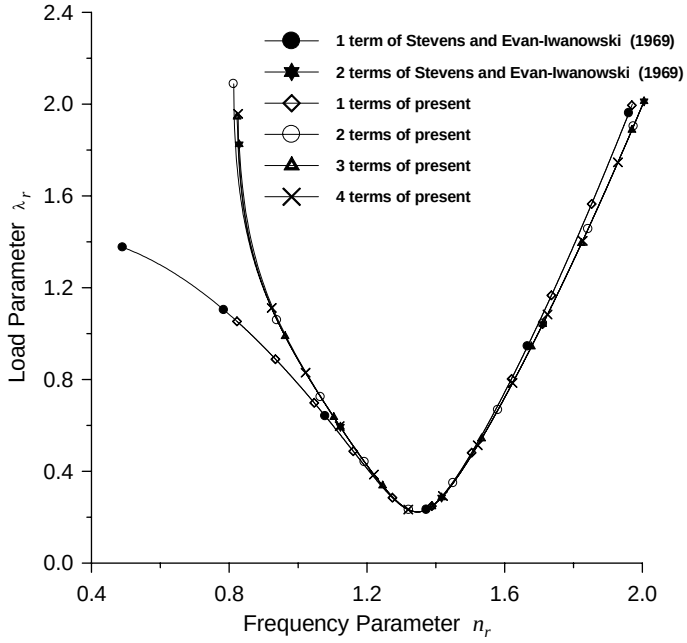

Fig. 3. Influence of the number of harmonic terms on the boundary of principal instability and comparison with Stevens and Evan-Iwanowski (1969) for $F_s/P_r^* = 0.48$.

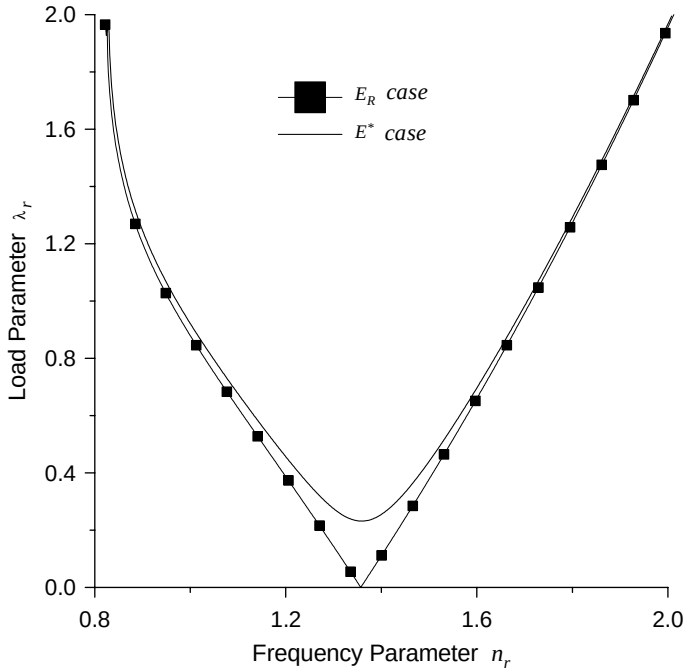

Fig. 4. Principal boundary of instability in the E_R and E^* cases for $F_s/P_r^* = 0.5$.

(1) The initial point is set to the minimum value of the excitation parameter, λ.
(2) The binary-search method is used to determine the vibrating frequency in Eq. (9), and the corresponding Ω. The frequency-dependent coefficients D and G, corresponding to the current frequency, are also obtained.
(3) Then, a point (Ω, λ) on the boundary of dynamic instability is obtained using the incremental harmonic balance method.
(4) When the corrective vector $\{R\}$ is not close to zero, steps 2 and 3 are repeated until the corrective vector $\{R\}$ is smaller than the convergence parameter.
(5) The parameter λ is increased by $\Delta\lambda$, and steps 2–4 repeated to locate the wanted point on the boundary of dynamic instability.

6. Numerical results and discussion

In this study, the boundaries of dynamic instability for the viscoelastic beam are determined. The viscoelastic material is considered to be as polymethyl methacrylate (Plexiglass) at room temperature. The length L of the beam is 445 mm (17.52 in.). The cross section of the beam is rectangular, with a width and thickness of 25.7 mm (1.01 in.) and 6 mm (0.236 in.), respectively. Polymethyl methacrylate (Plexiglass) has a density of 1190.2357 kg/m^3 (0.043 lb/in.^{3}), and a complex modulus, E^* that is a function of vibrating frequency. The real and imaginary parts of the complex modulus (Stevens and Evan-Iwanowski, 1969) have been presented as

$$E_R = a\omega^p; \quad \text{and} \quad E_I = b\omega^q \tag{21}$$

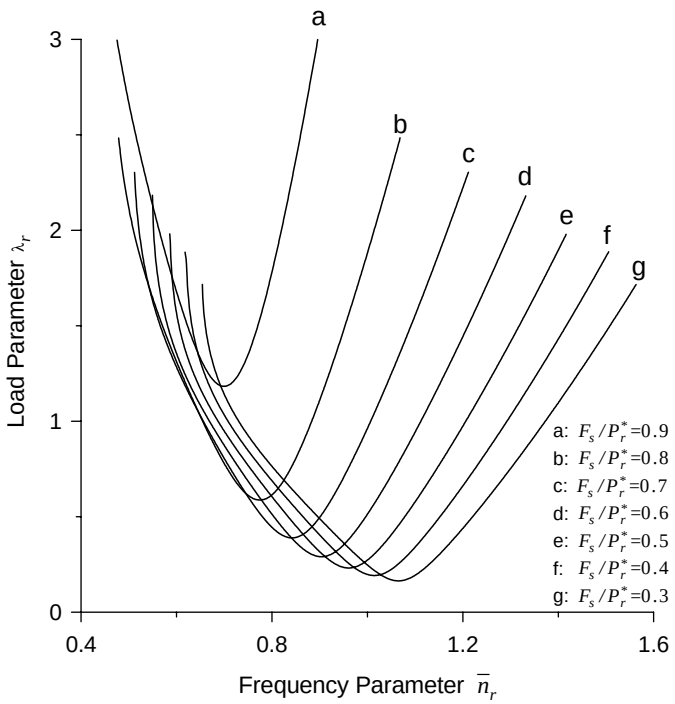

Fig. 5. Influence of the static force F_s on the boundary of principal instability.

where $a = 3.02\,\text{GPa}$ $(4.38 \times 10^5\,\text{psi})$, $b = 501.9383\,\text{MPa}$ $(7.28 \times 10^4\,\text{psi})$, $p = 0.0815$ and $q = -0.0635$. The complex modulus is validated over the frequency range 15–1000 Hz (100–6000 rad/s). In Eq. (21), the real part of the modulus increases with the frequency of vibration, but the imaginary part of the modulus decreases.

According to Eq. (7), the Euler critical load P_r^* is 72.95 N (16.4 lb) for the simply supported beam and the natural frequency of lateral vibration is $141.42(1 - F_s/P_r^*)^{1/2}$ rad/s.

Figs. 2 and 3 presents the principal boundaries of parametric instability with different numbers of harmonic terms for the different F_s/P_r^* ratios, obtained using the algorithms. The results are compared with the boundary of instability determined by Stevens and Evan-Iwanowski (1969). In Fig. 2, the boundary curves of the one-term approach and the two-term approach are consistent with the results of Stevens and Evan-Iwanowski (1969). The agreement between the results of the two-term approach in this study and the instability boundary obtained by Stevens and Evan-Iwanowski (1969) is good.

As shown in Figs. 2 and 3, a three-term approach gives highly accurate results. The curves of the instability boundary almost coincide with those of more harmonic terms, even for large values of the parameter of excitation, λ_r. The results of the three-term and four-term approaches converge. Formulating the equation of the instability boundary for large numbers of harmonic terms is difficult using the conventional method. The algorithms in this study easily and conveniently determine the boundary of parametric instability for any number of harmonic terms.

Now, the following two cases are considered one that involves the complex modulus E^*, and one that involves only the real part of the modulus, E_R $(E_I = 0)$. In both cases, the elastic modulus depends on the frequency of vibration. Fig. 4 compares the curves in the E_R and E^* cases, and the principal boundary of instability for the E^* case is shifted away from the $\mu_r = 0$ axis. This phenomenon shows the effect of the damping capacity of the viscoelastic material, and the loss factor presents the damping capacity of the material.

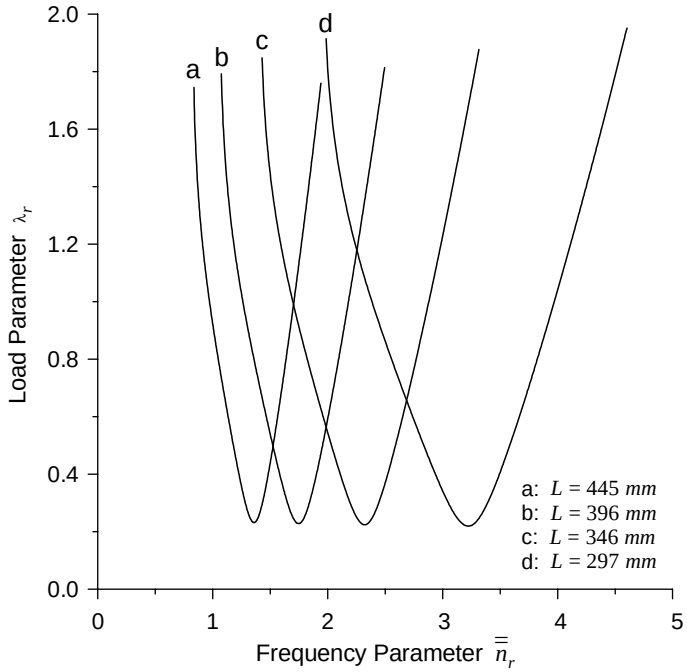

Fig. 6. Influence of the length of the beam on the principal boundary of instability for $F_s/P_r^* = 0.5$.

Fig. 5 plots the boundaries of principal instability under various static forces, F_s. Here, $\bar{n}_r^2 = \frac{\omega^2}{4\pi^4 E_r I/mL^4}$ is defined. Increasing the static force reduces the natural frequency and increases the loss factor. Therefore, the region of principal instability shifts away from the $\lambda_r = 0$ axis at low frequencies as the static force is increased.

The natural frequency of the beam is inversely proportional to L^2. The boundary of principal instability is at a frequency of the applied force that is double the fundamental natural frequency of the beam. The natural frequency of the beam increases as the length of the beam decreases. Herein, the parameter $\bar{\bar{n}}_r^2 = \frac{\omega^2}{4\pi^4 E_r I(1-F_s/P_r^s)/mL_0^4}$ and $L_0 = 445\,\text{mm}$ are defined. Consider a beam of length between 297 and 445 mm. Fig. 6 reveals that the frequency of the boundary of principal instability rises as the length of the beam decreases, but the loss factor changes little in this length range. The stiffness of the beam increases as the length of the beam decreases.

7. Conclusions

In this study, a simply supported viscoelastic beam is subjected to an axially harmonic load, whose complex modulus depends on the frequency of vibration. The principal dynamic instability is determined by combining the binary-search numerical procedure and the complex IHB method, modified by the authors into complex form. The results of this study agree closely with the results by Stevens and Evan-Iwanowski (1969). The boundary of parametric instability for any number of harmonic terms is easily, simply and conveniently determined. This new algorithm can determine the regions of dynamic instability of the complex Mathieu equation with frequency-dependent coefficients, for any engineering problem.

The numerical results indicate that the frequency influences the regions of dynamic stability. Additionally, an increase in the static force or the length of the beam has a stabilizing effect.

Appendix A

$$[C_1]_{mn} = \mathrm{Re}\left[\int_0^{2\pi} \left[-\Omega_0^2 n^2(\cos n\tau + \mathrm{i}\sin n\tau) + (1 + \mathrm{i}D - 2\lambda\cos 2\tau)(\cos n\tau + \mathrm{i}\sin n\tau)\right](\cos m\tau + \sin m\tau)\mathrm{d}\tau\right]$$

$$[C_2]_{mn} = \mathrm{Im}\left[\int_0^{2\pi} \left[-\Omega_0^2 n^2(\cos n\tau + \mathrm{i}\sin n\tau) + (1 + \mathrm{i}D - 2\lambda\cos 2\tau)(\cos n\tau + \mathrm{i}\sin n\tau)\right](\cos m\tau + \sin m\tau)\mathrm{d}\tau\right]$$

$$\{R_1\}_m = \mathrm{Re}\left[\int_0^{2\pi} \left\{-\left[\Omega_0^2 \frac{\mathrm{d}^2 f_0}{\mathrm{d}\tau^2} + (1 + \mathrm{i}D - \lambda_0\cos 2\tau) f_0\right](\cos m\tau + \sin m\tau)\right\}\mathrm{d}\tau\right]$$

$$\{R_2\}_m = \mathrm{Im}\left[\int_0^{2\pi} \left\{-\left[\Omega_0^2 \frac{\mathrm{d}^2 f_0}{\mathrm{d}\tau^2} + (1 + \mathrm{i}D - \lambda_0\cos 2\tau) f_0\right](\cos m\tau + \sin m\tau)\right\}\mathrm{d}\tau\right]$$

$$\{P_1\}_m = \mathrm{Re}\left[\int_0^{2\pi} (2\cos 2\tau f_0)(\cos m\tau + \sin m\tau)\mathrm{d}\tau\right]$$

$$\{P_2\}_m = \mathrm{Im}\left[\int_0^{2\pi} (2\cos 2\tau f_0)(\cos m\tau + \sin m\tau)\mathrm{d}\tau\right]$$

$$\{Q_1\}_m = \mathrm{Re}\left[\int_0^{2\pi}\left(-2\Omega_0\frac{\mathrm{d}^2 f_0}{\mathrm{d}\tau^2}\right)(\cos m\tau + \sin m\tau)\mathrm{d}\tau\right]$$

$$\{Q_2\}_m = \mathrm{Im}\left[\int_0^{2\pi}\left(-2\Omega_0\frac{\mathrm{d}^2 f_0}{\mathrm{d}\tau^2}\right)(\cos m\tau + \sin m\tau)\mathrm{d}\tau\right]$$

References

Bagley, R.L., Torvik, P.J., 1983. Fractional calculus—a different approach to analysis of viscoelastically damped structures. AIAA Journal 21 (5), 741–748.

Bolotin, V.V., 1964. The Dynamic Stability of Elastic Systems. Holdend-Day Inc., San Francisco, USA.

Burden, R.L., Faires, J.D., Reynolds, A.C., 1981. Numerical Analysis, second ed. Prindle, Weber and Schmidt Boston, Massachusetts, pp. 21–25.

Cederbaum, G., Mond, M., 1992. Stability properties of a viscoelastic column under a periodic force. Transactions of the ASME Journal of Applied Mechanics 59, 16–19.

Douglas, B.E., Yang, J.C.S., 1978. Transverse compressional damping in the vibratory response of elastic-viscoelastic beams. AIAA Journal 16 (9), 925–930.

Dovstam, K., 1995. Augmented Hooke's law in frequency domain: a three dimensional, material damping formulation. International Journal of Solids and Structures 32 (19), 2835–2852.

Golla, D.F., Hughes, P.C., 1985. Dynamics of viscoelastic structures—a time-domain, finite element formulation. Journal of Applied Mechanics 52 (4), 897–906.

Gurgoze, M., 1987. Parametric vibrations of a viscoelastic beam (Maxwell model) under steady axial load and transverse displacement excitation at one end. Journal of sound and Vibration 115 (2), 329–338.

Huang, S.C., Inman, D.J., Austin, E.M., 1996. Some design considerations for active and passive constrained layer damping treatments. Smart Materials and structures 5 (3), 301–313.

Johnson, C.D., Kienholz, D.A., 1981. Finite element prediction of damping in structures with constrained viscoelastic layers. AIAA Journal 20 (9), 1284–1290.

Kar, R.C., Ray, K., 1995. Dynamic stability of a pre-twisted, three layered, symmetric sandwich beam. Journal of Sound and vibration 183 (4), 591–606.

Kar, R.C., Sujata, T., 1991. Dynamic stability of a tapered symmetric sandwich beam. Computers & Structures 40 (6), 1441–1449.

Lau, S.L., Cheung, Y.K., Wu, S.Y., 1982. A variable parameter incrementation method for dynamic instability of linear and nonlinear elastic systems. Transactions of the ASME Journal of Applied Mechanics 49, 849–853.

Lesieutre, G.A., Bianchini, E., 1995. Time domain modeling of linear viscoelasticity using anelastic displacement fields. Journal of Vibration and Acoustics 117 (4), 424–430.

Lesieutre, G.A., Mingori, D.L., 1990. Finite element modeling of frequency-dependent material damping using augmenting thermodynamic fields. Journal of Guidance 13 (6), 1040–1050.

McTavish, D.J., Hughes, P.C., 1993. Modeling of linear viscoelastic space structures. Journal of Vibration and Acoustics 115, 103–110.

Pierre, C., Dowell, E.H., 1985. A study of dynamic instability of plates by an extended incremental harmonic balance method. Transactions of the ASME Journal of Applied Mechanics 52, 693–697.

Ray, K., Kar, R.C., 1995. Parametric instability of a sandwich beam under various boundary conditions. Computers & Structures 55 (5), 857–870.

Saito, H., Otomi, K., 1979. Parametric response of viscoelastically supported beams. Journal of sound and Vibration 63 (2), 169–178.

Shen, I.Y., 1995. Bending and torsional vibration control of composite beams through intelligent constrained-layer damping treatments. Smart Materials and Structures 4 (4), 340–355.

Shen, I.Y., 1996. Stability and controllability of Euler–Bernoulli beams with intelligent constrained layer treatments. Journal of Vibration and Acoustics 118 (1), 70–77.

Shirahatti, U.S., Sinha, S.C., 1994. On the stability of perfect viscoelastic columns. Journal of Sound and Vibration 174 (1), 57–68.

Steidel Jr., R.F., 1989. An introduction to mechanical vibrations, third ed. John Wiley and Sons, New York.

Stevens, K.K., 1969. Transverse vibration of a viscoelastic column with initial curvature under periodic axial load. Transactions of the ASME Journal of Applied Mechanics, 814–818.

Stevens, K.K., Evan-Iwanowski, R.M., 1969. Parametric resonance of viscoelastic columns. International Journal Solids Structures 5, 755–765.

Sun, C.T., Lu, Y.P., 1995. Vibration Damping of Structural Elements. Prentice Hall PTR, New Jersey, USA.

Szyszkowski, W., Glockner, P.G., 1985. The stability of viscoelastic perfect columns: a dymamic approach. International Journal of Solids and Structures 21 (6), 545–559.

Varadan, V.V., Lim, Y.H., Varadan, V.K., 1996. Closed loop finite-element modeling of active/passive damping in structural vibration control. Smart Materials and Structures 5 (5), 685–694.

Yiu, Y.C., 1993. Finite element analysis of structures with classical viscoelastic materials, In: Proceedings of the 34th AIAA/ASME/ASCE/AHS/ASC Structures, Structural Dynamics and Materials Conference, La Jolla, CA, April, 2110–2119.

Yiu, Y.C., 1994. Substructure and finite element formulation for linear viscoelastic materials, In: Proceedings of the 35th AIAA/ASME/ASCE/AHS/ASC Structures, Structural Dynamics and Materials Conference, Hilton Head, SC, April, 1585–1594.

Yuen, S.W., Lau, S.L., 1991. Effects of in-plane load on nonlinear panel flutter by incremental harmonic balance method. AIAA Journal 29 (9), 1472–1479.